PRAMANA
— journal of
physics

Vol. 64, No. 4
April 2005
pp. 563–575

Evolution of classical projected phase space density in billiards

DEBABRATA BISWAS
Theoretical Physics Division, Bhabha Atomic Research Centre, Mumbai 400 085, India
E-mail: malabika6@rediffmail.com

Abstract. The classical phase space density projected on to the configuration space offers a means of comparing classical and quantum evolution. In this alternate approach that we adopt here, we show that for billiards, the eigenfunctions of the coarse-grained projected classical evolution operator are identical to a first approximation to the quantum Neumann eigenfunctions. Moreover, there exists a correspondence between the respective eigenvalues although their time evolutions differ.

Keywords. Projected density; billiards; quantum correspondence.

PACS Nos 05.45.Mt; 03.65.Sq; 05.45.Ac

1. Introduction

The phase space density provides an alternate route for the study of classical dynamics that is both interesting and practical. Its evolution is governed by the Perron–Frobenius (PF) operator, $\mathcal{L}^t$,

$$\mathcal{L}^t \circ \rho(\mathbf{x}) = \int \delta(\mathbf{x} - \mathbf{f}^t(\mathbf{x}'))\rho(\mathbf{x}')\mathrm{d}\mathbf{x}', \tag{1}$$

where ρ refers to the phase space density, $\mathbf{x} = (\mathbf{q}, \mathbf{p})$ is a point in phase space and $\mathbf{f}^t(\mathbf{x})$ is its position at time t.

A knowledge of the spectral decomposition of $\mathcal{L}^t$ allows one to evaluate correlations, averages and other quantities of interest. In the Hilbert space of phase space functions, $\mathcal{L}^t$ is unitary [1,2]. Thus, the eigenvalues lie on the unit circle. The existence of an invariant density, ρ_0, implies $\mathcal{L}^t \circ \rho_0 = \rho_0$. Further, if the unit eigenvalue is non-degenerate, the system is ergodic. For integrable systems, the spectrum of $\mathcal{L}^t$ is discrete while for mixing systems, there is a continuous spectrum apart from the unit eigenvalue. The decay to the invariant density is connected to the continuous part of the spectrum. When the decay is exponential as in the case of a class of chaotic systems, the Fourier transforms of time-correlations have poles in the complex frequency plane or broad peaks (Ruelle–Pollicott resonances) along the real frequency axis, the positions of which are independent of the observable

chosen [3]. Techniques for the determination of the poles are now well-developed at least when the dynamics is purely hyperbolic.

While the eigenvalues of the Perron–Frobenius operator are reasonably well-studied, its eigenfunctions have not received as much attention. Apart from simple one-dimensional chaotic maps, the eigenfunctions of the Perron–Frobenius operator are hard to obtain even numerically while to the best of our knowledge, approximate solutions are not known. Part of the aim of this paper is to bridge this gap at least for the class of systems referred to as billiards.

A comparison of the classical and quantum dynamics using phase space densities is another aspect that has received attention [4–7]. A starting point for such a comparison is usually a quasi-probability distribution (QPD) as a quantum analog of the classical phase space density [6]. This enables one to 'lift' the quantum state to the phase space using the density operator, $\hat{\rho} = |\psi\rangle\langle\psi|$:

$$\rho_{(\Omega)}(q,p,t) = \frac{1}{(2\pi)^2}\int \mathrm{d}^2\xi\ \mathrm{e}^{\iota(\xi^* z^* + \xi z)\hbar}\mathrm{Tr}[\Omega\{\mathrm{e}^{-\iota\xi^*\hat{a}\dagger}\mathrm{e}^{-\iota\xi\hat{a}}\}\hat{\rho}]. \tag{2}$$

Here

$$z = (\sigma^{-1/2}q - \iota\sigma^{1/2}p)/(2\hbar) \tag{3}$$

$$\hat{a}^\dagger = (\sigma^{-1/2}\hat{q} - \iota\sigma^{1/2}\hat{p})/(2\hbar) \tag{4}$$

with $\sigma > 0$ while Ω refers to the ordering of $(\hat{q},\hat{p})$ that is chosen. A QPD resulting from anti-normal ordering

$$\Omega\{\mathrm{e}^{-\iota\xi^*\hat{a}\dagger}\mathrm{e}^{-\iota\xi\hat{a}}\} = \mathrm{e}^{-\iota\xi\hat{a}}\mathrm{e}^{-\iota\xi^*\hat{a}\dagger} \tag{5}$$

is the Husimi function which has been used in comparisons of classical and quantum evolutions. Note that the process of constructing a QPD is not unique and depends on the ordering scheme used to arrange the non-commuting operators $(\hat{q},\hat{p})$ [8,9]. Examples of other QPDs are the Wigner function and the Glauber–Sudarshan 'P' function [8].

The Husimi function, ρ_{H}, can be expressed as the diagonal matrix element of the density operator $\hat{p}$ with respect to a coherent state. The evolution of the Husimi function, ρ_{H}, is governed by the Liouville–von Neumann equation

$$\frac{\partial}{\partial t}\rho_{\mathrm{H}} = \mathcal{G}\rho_{\mathrm{H}} = -\iota\langle z|[\hat{H},\hat{\rho}]|z\rangle, \tag{6}$$

where $|z\rangle$ is the coherent state. While the eigenvalues of the Husimi propagator, $\mathcal{G}$, lie on the unit circle, coarse graining of phase space leads to loss of unitarity and hence lends itself to comparison with the eigenvalues of the Liouville operator. For the kicked top, the eigenvalues of the two operators have been found to be identical [6]. Coarse graining due to noise has also been considered [7] and it was found that the quantum spectrum converges to the classical one in the semiclassical limit for maps on the torus.

The primary aim of this paper is to compare classical and quantum evolutions using an alternate approach that is free from the uniqueness problems associated

with quasi-probability distributions. In the process, we shall also discover a means of evaluating classical eigenfunctions. In order to avoid the need to evaluate QPDs (i.e. the full phase distribution), we shall project the classical density to the configuration space by integrating out the momentum: $\rho(\mathbf{q}) = \int \rho(\mathbf{q}, \mathbf{p})\ \mathrm{d}\mathbf{p}$. We shall then compare the eigenstates of the projected Perron–Frobenius operator with the quantum eigenstates.

While we shall restrict ourselves to billiards here, the essential idea of seeking a quantum–classical correspondence using the projected density instead of the full phase space density is applicable to other systems as well. In the following, we shall show that for billiards, there exists a correspondence between the eigenvalues of the coarse-grained projected classical evolution operator ($\mathcal{L}_P^t$) and the quantum Neumann spectrum, while the respective eigenfunctions are identical to a first approximation.

The paper is organized as follows: In §2, we shall introduce billiards, the concept of polygonalization and the evolution operator for the projected density. We then show in §3 that a plane-wave superposition is a quantum Neumann eigenfunction and an eigenfunction of the classical projected evolution operator under identical conditions. Numerical demonstration of these results is provided in §4. Finally a summary and discussion of the results is provided in the concluding section.

2. The projected Perron–Frobenius operator for billiards

Apart from being a paradigm in the field of classical and quantum chaos, billiards have relevance in a variety of contexts. The Helmholtz equation describing the quantum billiard problem also describes acoustic waves, modes in microwave cavities and has relevance in studies on 'quantum wells', 'quantum corrals', mesoscopic systems and nanostructured materials. The Neumann boundary condition has important manifestation in acoustic waves, surface water waves, TE modes in cavities and modes of a drum with stress-free boundaries [10].

In a classical billiard, a particle moves freely inside an enclosure and reflects specularly from the boundary. Depending on its shape, billiards exhibit the entire range of behaviour observed in other dynamical systems. They also provide a means of coarse graining that is perhaps unique. The dynamics of smooth billiards can be coarse grained by polygonalizing the boundary [11–13]. Rational polygonal billiards are non-ergodic and non-mixing. However, the short-time dynamics of a polygonalized billiard can approximate that of the smooth billiard [11].

The quantum billiard problem consists of determining the eigenvalues and eigenfunctions of the Helmholtz equation

$$\nabla^2\psi(q) + k^2\psi(q) = 0 \tag{7}$$

with $\psi(q) = 0$ (Dirichlet) or $\hat{\mathbf{n}} \cdot \nabla\psi = 0$ (Neumann boundary condition; $\hat{\mathbf{n}}$ is the unit normal) on the boundary. Its semiclassical description holds the key to the quantum–classical correspondence. However, since a quantum state (or the quasi-probability distributions constructed out of it) can essentially resolve phase space structures of the size of a Plank cell, polygonalization provides just as much information about the quantum state at the semiclassical level [12,14].

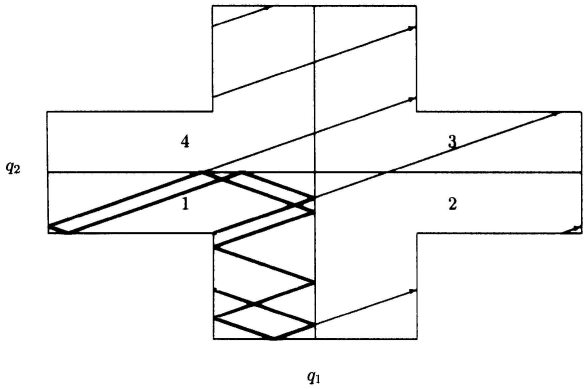

Figure 1. The singly connected invariant surface for an L-shaped billiard consists of four copies with edges appropriately identified. A trajectory originating near the $3\pi/2$ vertex in 1 is plotted in configuration space using bold lines and the corresponding unfolded trajectory is also shown. The latter consists of parallel segments and the trajectory can be parametrized by the angle φ that it makes for example with the q_1 axis.

Though polygonalization of billiard boundaries may not be essential as we shall demonstrate later, we shall nevertheless use it for establishing a connection between the eigenstates of the evolution operator for projected classical densities and the quantum eigenstates. The 'unfolded' dynamics of a polygonalized billiard can be viewed locally as a straight line on a singly connected invariant surface consisting of multiple copies of the enclosure glued together appropriately at the edges, each copy denoting a momentum direction that is related to the previous one by the law of reflection at the glued edge. Figure 1 provides an example of such a construction using the L-shaped billiard (see also [15,16]).

It is clear from the unfolded dynamics that the magnitude of the momentum (p) and the angle φ that $\mathbf{p}$ makes with a given axis are conserved. It is thus convenient to treat $\mathbf{p}$ in polar coordinates (p, φ). Transforming from (p_x, p_y) to (p, φ) and noting that p and φ are conserved in the unfolded picture, the $\mathbf{p}$ integration in eq. (1) simplifies as

$$\int \mathrm{d}p_x \mathrm{d}p_y \delta(p_x - p_x'^t(\mathbf{q}', \mathbf{p}'))\delta(p_y - p_y'^t(\mathbf{q}', \mathbf{p}'))h(\mathbf{q}', \mathbf{p}')$$
$$= \int \mathrm{d}\varphi\ \delta(\varphi - \varphi')h(\mathbf{q}'_{\mathbf{u}}, \varphi'; p) = h(\mathbf{q}'_{\mathbf{u}}, \varphi; p), \tag{8}$$

where $\mathbf{q_u}$ is a point on the unfolded space, $p'^t_{x(y)}(\mathbf{q}', \mathbf{p}')$ is the $x(y)$ component of the momentum at time t for the initial phase space coordinate $(\mathbf{q}', \mathbf{p}')$ and

$$h(\mathbf{q}'_{\mathbf{u}}, \varphi; p) = \delta(\mathbf{q_u} - \mathbf{q}'^t_{\mathbf{u}}(\mathbf{q}'_{\mathbf{u}}; \varphi, p))\rho(\mathbf{q}'_{\mathbf{u}}; \varphi, p). \tag{9}$$

Thus

$$\mathcal{L}^t \circ \rho = \int \mathrm{d}\mathbf{q}'_{\mathbf{u}}\ \delta(\mathbf{q_u} - \mathbf{q}'^t_{\mathbf{u}}(\mathbf{q}'_{\mathbf{u}}; \varphi, p))\rho(\mathbf{q}'_{\mathbf{u}}). \tag{10}$$

Note that the time evolution of ρ depends on φ through the kernel as $\mathbf{q}_\mathbf{u}'^t$ depends on both the initial position and momentum. Thus $\mathcal{L}^t = \mathcal{L}^t(\varphi)$.

Projection onto to the configuration space requires an integration over the angle φ. The time evolution of the projected density is thus given by

$$\begin{aligned}\mathcal{L}_P^t \circ \rho(\mathbf{q}) &= \frac{1}{2\pi}\int_0^{2\pi} \mathrm{d}\varphi\ \mathcal{L}^t(\varphi) \circ \rho(\mathbf{q}) \\ &= \frac{1}{2\pi}\int \mathrm{d}\mathbf{q}_\mathbf{u}'\mathrm{d}\varphi\ \delta(\mathbf{q}_\mathbf{u} - \mathbf{q}_\mathbf{u}'^t(\mathbf{q}_\mathbf{u}'; p, \varphi))\rho(\mathbf{q}'). \end{aligned} \tag{11}$$

3. Eigenvalues and eigenfunctions of $\mathcal{L}_P$

One way of determining the spectrum of $\mathcal{L}^t$ is by studying its trace. It can be shown that the trace of $\mathcal{L}_P^t$, expressed in terms of periodic orbits, can be related to the semiclassical quantum eigenvalues through the trace of the energy dependent Green's function [17]. While a formal correspondence between the quantum Neumann spectrum and the spectrum of $\mathcal{L}_P^t$ can be established following the above procedure, it really holds only for large eigenenergies $\{E_n\}$ in the semiclassical sense, at least in the case of polygonalized billiards [16–19]. For smaller values of E_n, the correspondence exists only if the delta function kernel is smoothened. In effect, this results in a coarse graining of the dynamics and in generic cases leads to the inclusion of terms in the classical trace which exist as higher order terms in the quantum trace formula. It may be noted that despite the smoothening, the restored correspondence is only approximate in generic cases as other quantum corrections exist.

For integrable polygons such as the rectangle, the correspondence between the spectrum of the projected Perron–Frobenius operator and the Neumann spectrum is exact and can be shown directly [16]. For that, it is simpler to work with action and angle coordinates. It is easy to see that the eigenfunctions and eigevalues of $\mathcal{L}^t$ are

$$\phi_\mathbf{n}(\theta_1, \theta_2) = \mathrm{e}^{\iota(n_1\theta_1 + n_2\theta_2)}, \tag{12}$$

$$\Lambda_\mathbf{n}(t) = \exp\{it(n_1\omega_1 + n_2\omega_2)\}, \tag{13}$$

where (n_1, n_2) are natural numbers. To illustrate this, we consider a rectangular billiard where the Hamiltonian expressed in terms of the actions, I_1, I_2 is $H(I_1, I_2) = \pi^2(I_1^2/L_1^2 + I_2^2/L_2^2)$ where L_1, L_2 are the lengths of the two sides. With $I_1 = \sqrt{E}L_1\cos(\varphi)/\pi$ and $I_2 = \sqrt{E}L_2\sin(\varphi)/\pi$, at a given energy, E, each torus is parametrized by a particular value of φ. Thus

$$\Lambda_\mathbf{n}(t;\varphi) = \mathrm{e}^{\iota 2\pi t\sqrt{E}(n_1\cos(\varphi)/L_1 + n_2\sin(\varphi)/L_2)} \tag{14}$$

and the spectrum of $\mathcal{L}^t$ is parametrized by φ. The eigenvalues of the projected operator, $\mathcal{L}_P^t$ are thus [16]

$$\frac{1}{2\pi}\int \mathrm{d}\varphi\ \Lambda_{\mathbf{n}}(t;\varphi) = J_0(\sqrt{E_{\mathbf{n}}}l), \tag{15}$$

where J_0 is the zeroth order Bessel function and $E_n = \pi^2(n_1^2/L_1^2 + n_2^2/L_2^2)$, n_1, n_2 being natural numbers. Thus

$$\mathcal{L}_P^t\ \mathrm{e}^{\iota(n_1\theta_1+n_2\theta_2)} = J_0(\sqrt{E_{\mathbf{n}}}l)\ \mathrm{e}^{\iota(n_1\theta_1+n_2\theta_2)}. \tag{16}$$

This gives us the correspondence between the eigenvalues of $\mathcal{L}_P^t$ and the quantum Neumann spectrum. In the following, we shall derive the correspondence between eigenvalues using an alternate prescription besides showing that the classical and quantum eigenfunctions are identical (see [13] for Dirichlet spectrum).

From the above discussion, it is obvious that despite the correspondence, quantum time evolution differs from evolution due to $\mathcal{L}_P^t$ as the eigenvalues evolve differently. The quantum Neumann eigenfunctions are however (approximate) eigenfunctions of $\mathcal{L}_P^t$ as well. As an illustrative example, consider a particle in a one-dimensional box and consider the evolution of the quantum Neumann eigenfunction $\psi_n(q) = \mathrm{e}^{\iota k_n q} + \mathrm{e}^{-\iota k_n q}$, $k_n = n\pi/L$. Its time evolution in quantum mechanics is simply $\mathrm{e}^{-\iota E_n t/\hbar}\psi(q)$ where $E_n = \hbar^2 k_n^2/2m$. To find the evolution under $\mathcal{L}_P^t$, note that in this one-dimensional case

$$\begin{aligned}\mathcal{L}_P^t &= \frac{1}{2}[\mathcal{L}^t(\varphi=0) + \mathcal{L}^t(\varphi=\pi)] \\ &= \frac{1}{2}[\mathcal{L}^t(+) + \mathcal{L}^t(-)],\end{aligned} \tag{17}$$

where $\mathcal{L}^t(\pm)$ refer to positive and negative velocities. The classical evolution for positive velocity, $\mathcal{L}^t(+)\circ\psi_n(q)$, is given by

$$(\mathrm{e}^{\iota k_n q^{-t}(+v)} + \mathrm{e}^{-\iota k_n q^{-t}(+v)}), \tag{18}$$

where $q^{-t}(+v)$ is the position at time $-t$ with initial position q and initial velocity $+v$. Similarly, $\mathcal{L}^t(-)\circ\psi_n(q)$ is

$$(\mathrm{e}^{\iota k_n (q^{-t}(-v))} + \mathrm{e}^{-\iota k_n (q^{-t}(-v))}) \tag{19}$$

with the $-$ sign in $\mathcal{L}^t(-)$ denoting negative velocity. Note that the flow is such that the velocity changes sign at every reflection from the walls at $q=0$ and $q=L$. For the flow $q^{-t}(+v)$, the reflections occur at $t_n^+ = (q+nL)/v$ so that for $t_0^+ < t < t_1^+$, $q^{-t}(+v) = v(t-t_0^+) = vt - q$. Similarly, for the flow $q^{-t}(-v)$, the reflections occur at $t_n^- = (L-q+nL)/v$ and for $t_0^+ < t < t_1^+$, $q^{-t}(-v) = L - v(t-t_0^-) = 2L - vt - q$. Hence, it follows that

$$\mathcal{L}^t(\pm)\circ\psi_n(q) = \mathrm{e}^{\iota k_n(-q\ \pm\ vt)} + \mathrm{e}^{-\iota k_n(-q\ \pm\ vt)} \tag{20}$$

for all t. Thus

$$\mathcal{L}_P^t \circ \psi_n(q) = \cos(k_n v t)\psi_n(q). \tag{21}$$

In other words, the quantum eigenfunction is also an eigenfunction of the projected classical evolution operator $\mathcal{L}_P^t$. For general polygonalized billiards, we shall

establish this by showing that the condition under which a plane-wave superposition is a quantum (semiclassical) eigenfunction is identical to the condition for this plane-wave superposition to be an eigenfunction of $\mathcal{L}_P^t$.

For polygonalized billiards, the semiclassical wave function can be expressed as

$$\psi(q) = \sum_{j=1}^{M} A_j \mathrm{e}^{\iota k \cos(\mu_j)x + \iota k \sin(\mu_j)y}, \tag{22}$$

where A_j are constants and the number of terms M in the expansion is determined by the closure of the wave vector $\vec{k} = (k\cos\mu_j, k\sin\mu_j)$ under reflection from all the edges [20]. For this finite superposition of plane waves, the Neumann boundary condition $\hat{\mathbf{n}} \cdot \nabla\psi = 0$ on ∂B can be satisfied if the waves vanish in pairs with an incident wave giving rise to a reflected wave. Thus on the lth segment, $y = a_l x + b_l$, of the polygonalized boundary, we must have

$$\begin{aligned} &A_j(n_x \cos\mu_j + n_y \sin\mu_j)\mathrm{e}^{\iota k\cos\mu_j x + \iota k \sin\mu_j y} \\ &+A_{j'}(n_x \cos\mu_{j'} + n_y \sin\mu_{j'})\mathrm{e}^{\iota k\cos\mu_{j'} x + \iota k \sin\mu_{j'} y} = 0, \end{aligned} \tag{23}$$

where $n_x = \cos(\theta_l)$ and $n_y = \sin(\theta_l)$ are the direction cosines of the outward normal to the lth segment and θ_l is the angle between the positive x-axis and the outward normal to the lth line segment.

Assuming that $\mu_{j'}$ is related to μ_j through the laws of reflection at the lth segment, it is easy to show that

$$\cos\mu_j + a_l \sin\mu_j = \cos\mu_{j'} + a_l \sin\mu_{j'}, \tag{24}$$

where a_l is related to θ_l through $a_l = -\cot(\theta_l)$ and $\mu_{j'} = \pi - \mu_j + 2\theta_l$. Thus, eq. (23) reduces to

$$A_j \mathrm{e}^{\iota b_l k \sin\mu_j} - A_{j'} \mathrm{e}^{\iota b_l k \sin\mu_{j'}} = 0. \tag{25}$$

Note that for each of the K segments on the boundary, the jth wave has in general a different reflected wave as a counterpart so that eq. (25) gives K different expressions for A_j. In general (barring exceptions such as the rectangle billiard), these 'boundary conditions' can be satisfied only approximately as we shall argue below. Recall that for the numerical determination of exact eigenvalues using a plane-wave basis, the boundary is discretized (N points) and an appropriate measure (such as a determinant) is used to determine the eigenstates which satisfy the boundary condition at these points. Convergence can be achieved by increasing N so that as $N \to \infty$, the boundary condition is satisfied exactly. In contrast, the number of terms in eq. (22) is fixed. Thus, if the exact eigenfunction contains additional plane waves, the boundary condition will be satisfied approximately and the plane-wave expansion of eq. (22) can only give an approximate quantum eigenfunction.

It now remains to be established that the (finite) plane-wave superposition (eq. (22)) is also an approximate eigenfunction of the evolution operator, $\mathcal{L}_P^t$, provided the set of 'quantization' conditions given by eq. (25) are satisfied.

Consider therefore the plane-wave superposition of eq. (22). Its evolution due to $\mathcal{L}^t(\varphi)$ is given by

$$\mathcal{L}^t(\varphi) \circ \psi_n(q) = \sum_{j=1}^{M} A_j \mathrm{e}^{\iota k_x x^{-t}(\varphi) + \iota k_y y^{-t}(\varphi)}, \tag{26}$$

where $k_x = k\cos(\mu_j)$, $k_y = k\sin(\mu_j)$ while $x^{-t}(\varphi)$ and $y^{-t}(\varphi)$ denote the flow at time $-t$ with initial position (x, y) and velocity $(v\cos\varphi, v\sin\varphi)$. For short times (no reflection), this is given by

$$\begin{aligned}\mathcal{L}^t(\varphi) \circ \psi_n &= \sum_{j=1}^{M} A_j \mathrm{e}^{\iota k_x (x - v\cos\varphi t) + \iota k_y (y - v\sin\varphi t)} \\ &= \sum_{j=1}^{M} A_j \mathrm{e}^{-\iota k v t \cos(\varphi - \mu_j)} \mathrm{e}^{\iota k_x x + \iota k_y y}. \end{aligned} \tag{27}$$

Thus

$$\mathcal{L}_P^t \psi_n(q) = \sum_j \frac{1}{2\pi} \int_{\mu_j}^{\mu_j + 2\pi} \mathrm{d}\varphi \mathrm{e}^{-\iota k v t \cos(\varphi - \mu_j)} \mathrm{e}^{\iota k_x x + \iota k_y y} \tag{28}$$

$$= J_0(kvt)\psi_n(q). \tag{29}$$

Note that there is no restriction on the allowed values of k so far and any plane-wave superposition is an eigenfunction. We shall now determine the evolution of a single wave after reflection from one of the segments, $y = a_l x + b_l$. For the flow, $(x^{-t}(\varphi), y^{-t}(\varphi))$, reflection from the line segment takes place at $t_0 = (x - x_0)/(v\cos\varphi) = (y - y_0)/(v\sin\varphi)$ where (x_0, y_0) is the point of impact. The flow at a time t after the reflection is given by

$$\begin{aligned} x^{-t}(\varphi) &= x(t) = x_0 + v\cos(\varphi - 2\theta_l)(t - t_0) \\ y^{-t}(\varphi) &= y(t) = y_0 - v\sin(\varphi - 2\theta_l)(t - t_0). \end{aligned} \tag{30}$$

It is possible to show that after one reflection from the segment $y = a_l x + b_l$, the wave $A_j \mathrm{e}^{\iota k \cos\mu_j x + k \sin\mu_j y}$ evolves quasi-classically to

$$A_{j'} \mathrm{e}^{\iota k \cos\mu_{j'}(x - v\cos\varphi t) + \iota k \sin\mu_{j'}(y - v\sin\varphi t)}, \tag{31}$$

where $\mu_{j'} = \pi - \mu_j + 2\theta_l$ and

$$A_{j'} = A_j \mathrm{e}^{\iota k b_l (\sin\mu_j - \sin\mu_{j'})}. \tag{32}$$

Note that the condition above for the new amplitude may be rewritten as

$$A_j \mathrm{e}^{\iota k b_l \sin\mu_j} - A_{j'} \mathrm{e}^{\iota k b_l \sin\mu_{j'}} = 0 \tag{33}$$

which is exactly the condition for the plane-wave superposition to be a quantum Neumann eigenfunction. Thus, after one reflection, the finite plane-wave superposition assumes the form for small t (eq. (27)) provided the reflected waves are included in the superposition. It follows that for the set $\{k_n\}$ for which conditions in eq. (25) are satisfied, $\psi_n(q)$ is an eigenfunction of the projected evolution operator:

$$\begin{aligned}\mathcal{L}_P^t \circ \psi_n(q) &= \frac{1}{2\pi}\int \mathrm{d}\varphi\ \mathcal{L}^t(\varphi)\psi_n(q)\\ &= \frac{1}{2\pi}\sum_j \int \mathrm{d}\varphi\ \mathrm{e}^{-\iota k_n v t\cos(\varphi-\mu_j)} A_j \mathrm{e}^{\iota S_j(k_n)}\\ &= J_0(k_n v t)\psi_n(q), \end{aligned} \tag{34}$$

where $S_j(k_n) = k_n\cos(\mu_j)x + k_n\sin(\mu_j)y$ and J_0 is the Bessel function. We have thus used an alternate means of arriving at the eigenvalues of $\mathcal{L}_P^t$.

4. Numerical evidence

We now present our numerical results. The chaotic stadium-shaped billiard that we consider, consists of two parallel straight segments of length 2 joined on either end by a semicircle of unit radius. The polygonalized version has 10 segments approximating the semicircle.

In order to determine the eigenvalues and eigenfunctions of $\mathcal{L}_P^t$, we shall evaluate its smoothened kernel

$$\begin{aligned}K_P(\mathbf{q},\mathbf{q}',t) &= \frac{1}{2\pi}\int_0^{2\pi} \mathrm{d}\varphi\ \delta_\epsilon(\mathbf{q}-\mathbf{q}'^t(\varphi))\\ &= \sum_n \psi_n(\mathbf{q})\psi_n^*(\mathbf{q}')\Lambda_n(t)\end{aligned} \tag{35}$$

as a function of time. Here $\Lambda_n(t) = J_0(k_n v t)$ and δ_ϵ is a smoothened delta function and $\psi_n(\mathbf{q})$ are the eigenfunctions of the projected Perron–Frobenius operator, $\mathcal{L}_P^t$. As an example of the smoothened delta function, we consider the hat function which is zero outside a cell of size ϵ [21,22]. The φ integration is performed by shooting trajectories from a point $\mathbf{q}'$ at various angles and evaluating the fraction of trajectories in a cell of size ϵ at $\mathbf{q}$ [16]. For the numerical results presented here $\epsilon \simeq 0.04$ and the number of trajectories used for the φ integration is 40000. Figure 2 shows an example of polygonalization and the arbitrary trajectory shooting algorithm.

As $\Lambda_n \sim \cos(\sqrt{E_n}t - \pi/4)$ for $v = 1$, the kernel K_P is a sum of oscillatory terms. A Fourier transform of $K_P(\mathbf{q},\mathbf{q}',t)$ thus has peaks at $k = \sqrt{E_n}$, the width

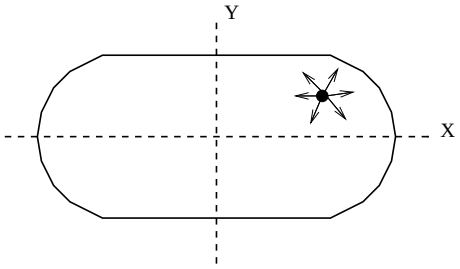

Figure 2. A polygonalized stadium. The algorithm consists of shooting trajectories from a cell and measuring the fraction inside at any time t.

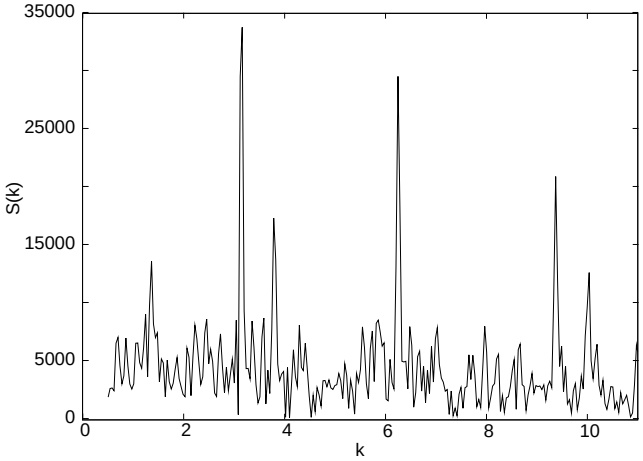

Figure 3. Fourier transform of the kernel $K_P(q, q, t)$ for a polygonalized stadium. The significant peaks correspond to $\sqrt{E_n}$. To measure the eigenfunction of $\mathcal{L}_P$, the point q is varied.

depending on ϵ and the heights on $\psi_n(\mathbf{q})$. An eigenfunction corresponding to a particular eigenvalue can thus be measured by varying $\mathbf{q}$ and measuring the height of the desired peak at each point. A typical Fourier transform is shown in figure 3.

Figure 4a shows the eigenfunction of $\mathcal{L}_P^t$ corresponding to the first peak at a non-zero k ($k \simeq 0.70$) in the power spectrum of the (smoothened) kernel $K_P(\mathbf{q}, \mathbf{q}, t)$ for the polygonalized stadium. Only the first quadrant is shown due to the reflection symmetry of the system. Note that we have plotted the intensities as the peak heights are proportional to $|\psi_n(q)|^2$. Figure 4b shows the corresponding quantum Neumann eigenfunction of the smooth stadium at $k \simeq 0.87$ found using the boundary integral technique. Figure 4c is similar to figure 4a but for a smooth stadium. Clearly, polygonalization appears unimportant for observing the quantum–classical correspondence though it is useful for establishing the existence of the correspondence.

We next consider an excited 'bouncing ball' state in the smooth stadium. Figure 5a shows such an eigenstate of $\mathcal{L}_P^t$ obtained by measuring the peak $k = 6.328$. Figure 5b shows the quantum Neumann eigenfunction at $k = 6.37$. It is again clear that the quantum Neumann eigenfunction approximates the eigenfunction of $\mathcal{L}_P^t$. We have found this to be true for several eigenfunctions of the stadium and other billiards.

We have thus seen that there is a correspondence, albeit approximate, between the eigenstates of the quantum and projected classical evolution operators. The theoretical basis (see also [16]) clearly indicates that the eigenstates obtained using this method are at best 'semiclassical' in nature. In cases where the corrections are zero (rectangle or equilateral billiard), the quantum Neumann eigenstates are identical to the eigenstates of $\mathcal{L}_P$ and the smoothening parameter ϵ can be made small. In general, at higher energies, the peaks in the Fourier transform of $K_P(\mathbf{q}, \mathbf{q}', t)$ are generally harder to resolve as the density of eigenvalues increases with k. Thus, measuring projected eigenfunctions using trajectories becomes harder.

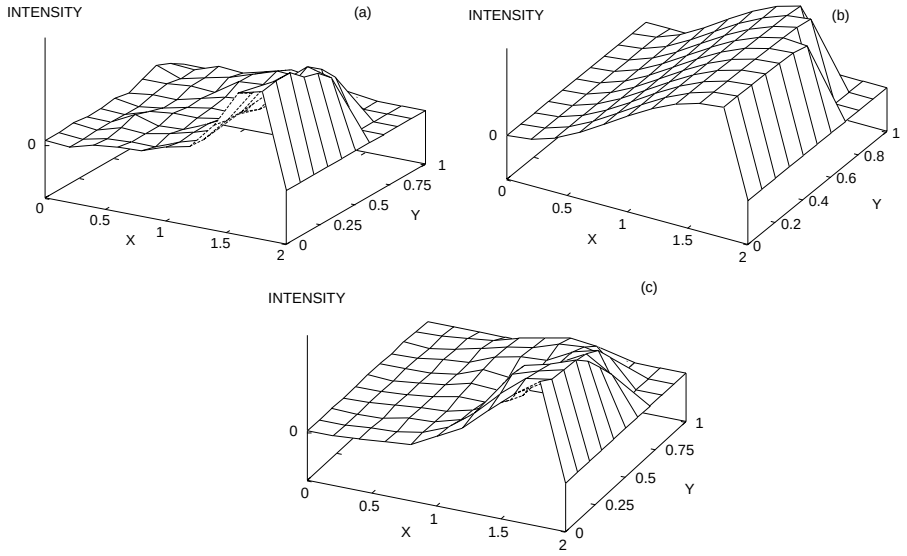

Figure 4. (**a**) An eigenfunction of $\mathcal{L}_P^t$ corresponding to the first non-zero eigenvalue of the polygonalized stadium. It is symmetric in y (Neumann) and antisymmetric in x (Dirichlet). (**b**) Its quantum counterpart in smooth stadium, (**c**) similar to figure 4a but for the smooth stadium.

There are basic differences in the interpretations of the quantum and projected classical eigenstates. Each quantum eigenfunction is associated with a density which is invariant in time while only the constant eigenfunction of $\mathcal{L}_P^t$ qualifies as a configuration space density and is invariant. All other densities, $\rho(\mathbf{q})$, decay to the invariant density on evolving with $\mathcal{L}_P^t$. The eigenvalues of $\mathcal{L}_P^t$ thus form a decay spectrum. The time evolution of a projected density can be expressed in terms of the eigenstates of $\mathcal{L}_P^t$ as

$$\rho(\mathbf{q},t) \simeq \rho_{\rm av} + \frac{1}{t^{1/2}} \sum_{n=1}^{\infty} c_n \psi_n(\mathbf{q}) \cos(\sqrt{E_n}t - \pi/4) \tag{36}$$

for t sufficiently large. The coefficients, $\{c_n\}$, apart from some factors, depends on $\int \psi_n(\mathbf{q})\rho(\mathbf{q},0)\mathrm{d}\mathbf{q}$. The approach to the uniform density, $\rho_{\rm av}$, is highly oscillatory and the overall decay rate may differ from $t^{-1/2}$ due to the sum of oscillatory terms. However, the locally time-averaged density has been found to agree with the form $a + b/t^{1/2}$ [17].

5. Discussion and conclusions

A discussion on coarse-graining is important to understand the significance of the result. There are two levels at which this has been carried out. Polygonalization is one of the methods of coarse-graining short time dynamics. As the number of

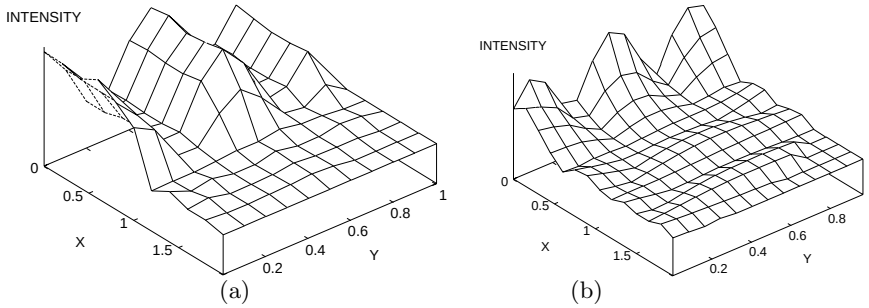

Figure 5. (**a**) An eigenfunction of $\mathcal{L}_P^t$ at $k = 6.33$ of the smooth stadium billiard shown in the first quadrant. It is symmetric in x and y. It has the structure of a bouncing ball mode. (**b**) Its quantum counterpart with $k \simeq 6.37$.

segments can be increased to approximate the smooth billiard arbitrarily well, it might be expected that the eigenvalues and eigenfunctions converge to those of the smooth billiard in both the quantum and classical case. Indeed, our numerical studies for the stadium (and lemon; results not presented here) billiard show this to be true for the classical eigenfunctions. Thus, coarse-graining via polygonalization appears unimportant for observing the correspondence.

Polygonalization nevertheless has an important use in the present study. It puts all billiards on the same footing and enables us to connect the quantum and classical eigenvalues and eigenfunctions analytically. A derivation for smooth billiards without invoking the polygonalization approximation is however desirable.

The second and more significant coarse-graining of the dynamics is related to the smoothening of the delta function kernel. This enables us to connect the classical and quantum eigenvalues even for smaller values of λ_n and is hence indispensable.

It is worth noting that the determination of exact eigenstates of the Perron–Frobenius operator is generally non-trivial while quantum states are easier to determine. The usefulness of the results presented here thus lies in using quantum states to evolve classical configuration space densities.

References

[1] A Lasota and M MacKey, *Chaos, fractals, and noise; stochastic aspects of dynamics* (Springer-Verlag, Berlin, 1994)
[2] P Gaspard, *Chaos, scattering and statistical mechanics* (Cambridge University Press, 1998)
[3] M Pollicott, *Invent. Math.* **81**, 413 (1985)
D Ruelle, *Phys. Rev. Lett.* **56**, 405 (1986)
[4] M Sano, *Phys. Rev.* **E59**, R3795 (1999)
[5] D Braun, *Chaos* **9**, 730 (1999)
[6] C Manderfeld, J Weber and F Haake, *J. Phys.* **A34**, 9893 (2001)
[7] S Nonnenmacher, *Nonlinearity* **16**, 1685 (2003)
[8] R R Puri, *Mathematical methods of quantum optics* (Springer, Berlin, 2001)
[9] W Zhang, D Feng and R Gilmore, *Rev. Mod. Phys.* **62**, 867 (1990)

[10] T A Driscoll and H P W Gottlieb, *Phys. Rev.* **E68**, 016702 (2003)
H-J Stockmann, *Quantum chaos – An introduction* (Cambridge University Press, Cambridge, 1999)
[11] J L Vega, T Uzer and J Ford, *Phys. Rev.* **E48**, 3414 (1993)
[12] D Biswas, *Phys. Rev.* **E61**, 5073 (2000)
[13] D Biswas, *Phys. Rev.* **E67**, 026208 (2003)
[14] The degree of polygonalization depends on the de Broglie wavelength, λ; see [12]
[15] D Biswas, *Phys. Rev.* **E61**, 5129 (2000)
[16] D Biswas, *Phys. Rev.* **E63**, 016213 (2001)
[17] D Biswas, *Phys. Rev. Lett.* **93**, 204102 (2004)
[18] D Biswas and S Sinha, *Phys. Rev. Lett.* **70**, 916 (1993)
[19] D Biswas, *Phys. Rev.* **E54**, R1044 (1996)
[20] E J Heller, *Phys. Scr.* **40**, 354 (1989)
J L Vega, T Uzer and J Ford, *Phys. Rev.* **E52**, 1490 (1995)
D Biswas and S Sinha, *Phys. Rev.* **E60**, 408 (1999)
[21] The smoothening parameter $\epsilon \sim \mathcal{O}(1/k_{\max})$ where $k_{\max}$ is the largest eigenvalue of interest [16]
[22] The hat function is appropriate as the eigenfunctions we are interested in belong to the Hilbert space. One may also use other smoothened delta functions